# Photon-mediated spin-mixing dynamics

Gregory S. Bentsen, Emily J. Davis, Lukas Homeier, Avikar Periwal, Eric Cooper, et al.

Gregory S. Bentsen, Emily J. Davis, Lukas Homeier, Avikar Periwal, Eric Cooper, Katherine Van Kirk, Monika H. Schleier-Smith, "Photon-mediated spin-mixing dynamics," Proc. SPIE 10934, Optical, Opto-Atomic, and Entanglement-Enhanced Precision Metrology, 109342P (1 March 2019); doi: 10.1117/12.2515795

SPIE.

Event: SPIE OPTO, 2019, San Francisco, California, United States

Invited Paper

# Photon-mediated spin-mixing dynamics

Gregory S. Bentsen, Emily J. Davis, Lukas Homeier, Avikar Periwal, Eric Cooper, Katherine Van Kirk, and Monika H. Schleier-Smith

*Department of Physics, Stanford University, Stanford, California 94305, USA*

## ABSTRACT

We analyze the dynamics of spin-mixing interactions generated by coupling spin-1 atoms to the mode of a high-finesse optical cavity. We show that the dynamics can be understood in terms of generators of the non-compact Lie group SU(1, 1) and introduce a set of SU(1, 1) coherent states which are preserved under Hamiltonian evolution. In terms of these coherent states the resulting dynamics may be interpreted as classical motion on the unit disk. We explicitly compute the trajectories of this classical motion and show that the motion is equivalent to spin-nematic squeezing in the atomic ensemble. Dissipation due to photon loss and non-uniform coupling between the atomic ensemble and the cavity mode lead to departures from this simple behavior. We introduce toy models that capture these experimental imperfections and solve them exactly.

**Keywords:** Light-matter interaction, spin-mixing dynamics, quantum entanglement, quantum metrology

## 1. INTRODUCTION

Engineering spin-dependent interactions between cold atoms has provided a powerful and versatile set of tools for studying the dynamics of many interacting quantum degrees of freedom and harnessing these interactions for quantum state preparation. In particular, collisional interactions in spinor Bose-Einstein condensates (BECs)[1] have been used to engineer parametric amplification of quantum noise[2,3] leading to the production of spin-nematic squeezed states with applications to quantum-enhanced metrology.[4,5] Interacting spinor Bose gases also feature a rich phase diagram, whose exploration has allowed for a detailed study of quantum phase transitions,[6–8] observation of dynamical effects such as the quantum Kibble-Zurek mechanism,[9] and adiabatic preparation of metrologically useful ground states.[10]

Recently, it has been demonstrated that similar spin-mixing dynamics are also accessible in cavity QED setups[11] in which the spin-mixing interactions are mediated by photons in the mode of an optical cavity.[12] Interactions achieved in this manner present a number of advantages over the collisional BEC approach. Since the interactions are mediated by a driven cavity mode that generates all-to-all pairwise interactions between atoms, the spin-mixing process occurs on much faster timescales than in collisional BEC experiments. Moreover, due to the high degree of tunability in cavity QED systems, one has access to the entire phase space, including both ferro- and antiferromagnetic phases, within a single experiment. By contrast, since the scattering lengths in spinor Bose gases are largely determined by the choice of atomic species, one must build separate experiments with different atomic species in order to explore the ferro- and anti-ferromagnetic phases. Finally, whereas collisional interactions are inherently short-ranged, cavity QED platforms are flexible enough to allow for novel extensions to the spin-mixing interactions, including generating 'infinite-range' all-to-all interactions, as well as breaking the all-to-all symmetry to allow for exotic sparse interaction structures between selected pairs of atoms.

Here we discuss the spin-mixing dynamics generated by the cavity QED system as observed by Davis, *et al.*[11] We develop complementary pictures of the dynamics using SU(1, 1) coherent states and squeezed states. We compute analytic expressions for the maximum squeezing achievable in the presence of dissipation. We also discuss extensions to the uniform spin-mixing model, including the case of non-uniform coupling to the cavity mode.

Send correspondence to gbentsen@stanford.edu

Optical, Opto-Atomic, and Entanglement-Enhanced Precision Metrology, edited by Selim M. Shahriar, Jacob Scheuer, Proc. of SPIE Vol. 10934, 109342P · © 2019 SPIE · CCC
code: 0277-786X/19/$18 · doi: 10.1117/12.2515795

## 2. SPINOR DYNAMICS IN CAVITY QED

Recently, Davis *et al.* experimentally demonstrated a scheme to generate spin-spin interactions between pairs of spin-1 atoms mediated by the mode of an optical cavity.[11] Upon integrating out the cavity mode, the coherent interactions between atoms may be described by an effective Hamiltonian

$$H = \chi \sum_{i,j=1}^{N} \xi_i \xi_j S_i^+ S_j^- + \sum_i h_i S_i^z + q \sum_i (S_i^z)^2 \tag{1}$$

where $\vec{S}_i$ are spin-1 operators representing the internal state of each atom $i$, $\chi$ is the interaction strength set by the intensity and detuning of the drive light, and $h_i, q$ are linear and quadratic Zeeman shifts, respectively. The coefficients $\xi_i$ arise from non-uniform coupling of the atoms to the cavity mode and can additionally be controlled by spatially inhomogeneous drive light from the side of the cavity. In addition, light leakage from the cavity mode generates a pair of relaxation operators:

$$L_\pm = \sqrt{\gamma_\pm} \sum_i \xi_i S_i^\pm \tag{2}$$

which induce dissipative spin-flips in the ensemble at the rates $\gamma_\pm$.

In addition to generating 'flip-flop' interactions between atoms that cause spin excitations to 'hop' between distant sites,[11] the above Hamiltonian also naturally generates 'spin-mixing' interactions, similar to those observed in spinor BEC experiments.[1–5] To see this, we assume uniform coupling $\xi_i = 1, h_i = h$ for simplicity, and introduce the mode operators $a_\pm, a_0$ to represent the atomic populations in the Zeeman states $|1, \pm 1\rangle, |1, 0\rangle$, respectively. In terms of these modes, the spin-spin Hamiltonian (1) may be written:

$$\begin{aligned} H = {} & 2\chi \left[ a_0^\dagger a_0^\dagger a_+ a_- + a_0 a_0 a_+^\dagger a_-^\dagger + a_+^\dagger a_+ (1 + a_0^\dagger a_0) + a_0^\dagger a_0 (1 + a_-^\dagger a_-) \right] \\ & + \frac{1}{2} h a_+^\dagger a_+ - \frac{1}{2} h a_-^\dagger a_- + q(a_+^\dagger a_+ + a_-^\dagger a_-). \end{aligned} \tag{3}$$

If we prepare all $N$ atoms in the state $|1, 0\rangle$, the Hamiltonian depletes the population in the *pump mode* $a_0$ and creates pairs of entangled excitations in the *side modes* $a_\pm$. This process is analogous to the parametric amplification dynamics that has been observed in spinor BECs.

Initially, the pump mode $a_0$ is macroscopically occupied, so we may treat it approximately as a classical field with occupation $a_0^\dagger a_0 \approx |\zeta|^2$ where $\zeta$ is a fixed $c$-number. This approximation is only valid for short times, however: since the total excitation number $M = a_+^\dagger a_+ + a_-^\dagger a_- + a_0^\dagger a_0$ is exactly conserved by the full Hamiltonian, treating $a_0^\dagger a_0$ as both classical and time-independent is only valid at short interaction times, before the occupation of the side modes $a_\pm$ causes significant depletion of the pump mode $a_0$. With these caveats in mind, we make the replacement $a_0 \to \zeta$ and pass into a rotating frame with respect to $H_0 = (2\chi - h)(a_+^\dagger a_+ - a_-^\dagger a_-)/2 - \chi - q$ to arrive at the effective Hamiltonian:

$$H = \Omega^* a_+ a_- + \Omega a_+^\dagger a_-^\dagger + \omega(a_+^\dagger a_+ + a_-^\dagger a_- + 1) \tag{4}$$

where $\Omega = 2\chi\zeta^2$ and $\omega = \chi(1 + 2|\zeta|^2) + q$. The result is recognizable as a two-mode squeezing Hamiltonian[13] whose dynamics are well-understood. For our purposes it will be advantageous to perform a coordinate rotation to a new pair of mode operators $c, d$:

$$\begin{aligned} a_+ &= (c - id)/\sqrt{2} \\ a_- &= (c + id)/\sqrt{2}. \end{aligned}$$

Written in terms of these new modes, the Hamiltonian splits into a pair of non-interacting terms:

$$\begin{aligned} H &= H_c + H_d \\ &= \frac{\Omega^*}{2} cc + \frac{\Omega}{2} c^\dagger c^\dagger + \omega(c^\dagger c + 1/2) + \frac{\Omega^*}{2} dd + \frac{\Omega}{2} d^\dagger d^\dagger + \omega(d^\dagger d + 1/2). \end{aligned} \tag{5}$$

Likewise, the relaxation operators now take the form:

$$L_{\pm} = \sqrt{\gamma_{\pm}} \left( \zeta c^{\dagger} + \zeta^{*} c \pm i \zeta d^{\dagger} \pm i \zeta^{*} d \right). \tag{6}$$

Each Hamiltonian $H_{c,d}$ is now recognizable as a single-mode squeezing Hamiltonian, which generates squeezing independently in the pair of phase spaces spanned by the modes $c, c^{\dagger}$ and $d, d^{\dagger}$. For the moment we consider the squeezing dynamics of $H$ in the absence of dissipation, but will return to analyze the dissipative dynamics in Section 4.

## 3. SPIN-NEMATIC SQUEEZING AND SU$(1,1)$

The dynamics of single-mode squeezing Hamiltonians $H_{c,d}$ is well-understood.[13] In particular, one can perform a Bogoliubov transformation in the operators $c, c^{\dagger}$ or $d, d^{\dagger}$ to diagonalize the Hamiltonians $H_c, H_d$, respectively, and solve for the spectrum exactly. Here, however, we will pursue a different approach that we believe more clearly illuminates the physics and allows for more rapid computation of quantities of interest. This approach is based on introducing a set of coherent states for the Lie group SU$(1,1)$,[14–16] similar to the more familiar coherent spin states (CSS)[17] used in the cold-atom and trapped-ion communities to describe the internal collective states of atoms.

To develop this framework, it suffices to restrict our attention to the dynamics of a single mode $c$ as it evolves under the single-mode squeezing Hamiltonian $H_c$. We introduce the bilinear operators:

$$K_z = \frac{1}{2} \left( c^{\dagger} c + \frac{1}{2} \right) \tag{7a}$$

$$K^{+} = \frac{1}{2} c^{\dagger} c^{\dagger} = (K^{-})^{\dagger} \tag{7b}$$

which form a closed SU$(1,1)$ algebra:[15,18]

$$[K_z, K^{\pm}] = \pm K^{\pm}$$
$$[K^{+}, K^{-}] = -2K_z.$$

In terms of these bilinears,

$$\begin{aligned} H_c &= \Omega K^{+} + \Omega^{*} K^{-} + 2\omega K_z \\ &= \vec{M} \cdot \vec{K} \end{aligned} \tag{8}$$

where $\vec{K} = (K_x, K_y, K_z)$, with $K_x = (K^{+} + K^{-})/2$, $K_y = (K^{+} - K^{-})/2i$, and

$$\vec{M} = 2\langle \mathrm{Re}\ \Omega, \mathrm{Im}\ \Omega, \omega \rangle.$$

Written in this language, the Hamiltonian (8) resembles a 'spin' $\vec{K}$ precessing in a 'magnetic field' $\vec{M}$. The 'spin' $\vec{K}$ in this case is an object that transforms under the Lie group SU$(1,1)$, similar to the way in which an angular momentum variable $\vec{S}$ transforms under the Lie group SU$(2)$. The similarities between these two Lie groups suggests that some of the tools and intuition we have for SU$(2)$ might be equally applicable to SU$(1,1)$. For example, for an SU$(2)$ spin $\vec{S}$ precessing in a real magnetic field $\vec{B}$, the physics is made particularly transparent by introducing a set of coherent spin states (CSS) $|\theta, \phi\rangle$. As illustrated in Fig. 1, these states are completely specified by a single unit vector $\vec{v}(\theta, \phi)$ on the Bloch sphere, whose components immediately give the expectation values of the spin operators: $\langle \vec{S} \rangle = \sqrt{s(s+1)}\ \vec{v}$, where $s$ is the quantum number labelling the representations of SU$(2)$, with $\vec{S}^2 = s(s+1)$. Moreover, these coherent states evolve simply under SU$(2)$ dynamics: in particular, in the presence of a magnetic field $\vec{B}$ the vector $\vec{v}$ simply precesses about the axis $\hat{B}$ at a rate proportional to $|B|$.

The analogy to SU$(2)$ dynamics suggests that one might be able to benefit in similar ways by introducing a set of coherent states for SU$(1,1)$. In particular, just as an SU$(2)$ Hamiltonian simply rotates spin-coherent states around on the Bloch sphere, we anticipate that the SU$(1,1)$ Hamiltonian (8) might simply translate the SU$(1,1)$ coherent states around in some other space.

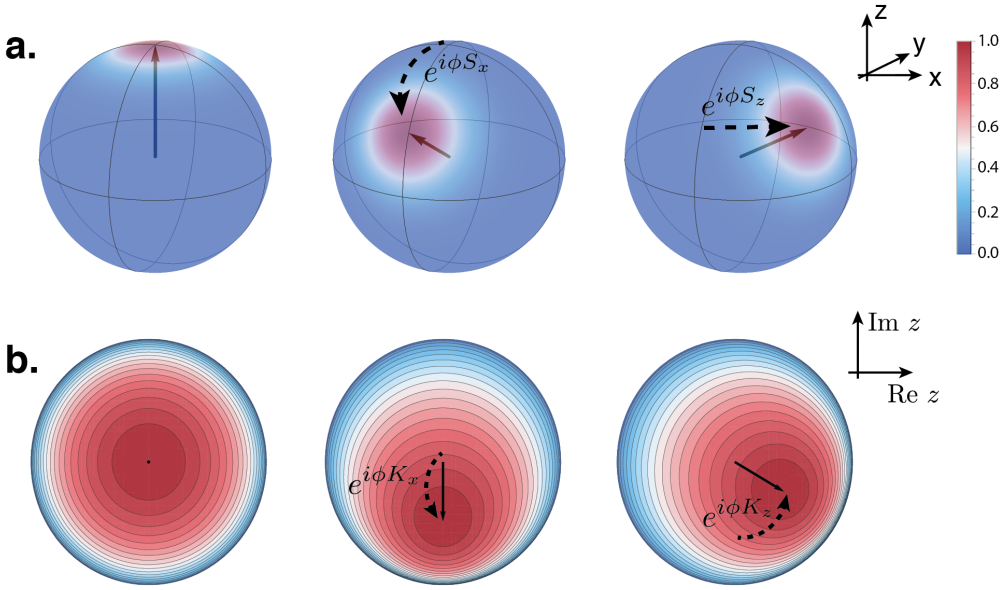


Figure 1. SU(2) and SU(1, 1) coherent states. (a) SU(2) coherent states are parameterized by a unit vector $\vec{v}$ (black arrow) on the Bloch sphere. Starting from a polarized state in the $S_z$ direction, we may apply rotations about the $S_x$ and $S_z$ axes, respectively, to obtain other spin-coherent states. Colors indicate the (unnormalized) Husimi Q distribution $H(\theta, \phi) = |\langle \theta, \phi | \psi \rangle|^2$, plotted for $s = 20$. (b) Similarly, SU(1, 1) coherent states are parameterized by a single complex number $z$ (black arrow) on the unit disk. Starting from the vacuum state $|0, k\rangle$, we may apply the generators $K_x, K_z$ to translate and rotate the coordinate $z$, respectively, to obtain other SU(1, 1) coherent states. Colors indicate the Husimi Q distribution $H(z) = |\langle z, k | \psi \rangle|^2$, plotted for $k = 1/4$.

### 3.1 SU(1, 1) Coherent States

Following Perelomov and others,[14–16] we define a set of SU(1, 1) coherent states using a 'displacement' operator $\mathcal{D}(z)$ parameterized by a single complex number $z$:

$$|z, k\rangle = \mathcal{D}(z) |0, k\rangle = e^{zK^+} e^{\ln(1-|z|^2)K_z} e^{-z^* K^-} |0, k\rangle \tag{9}$$

where the 'vacuum' state $|0, k\rangle$ is the uniquely-defined eigenstate of $K_z$ with $K_z |0, k\rangle = k |0, k\rangle$. The constant $k$ is called the Bargmann index and labels the representations of SU(1, 1), similar to the way that the quantum number $s$ for the total spin $\vec{S}^2 = s(s + 1)$ labels the representations of SU(2). In particular, $k$ labels the eigenvalues of the SU(1, 1) Casimir operator:

$$C_0 = K_z^2 - \frac{1}{2}\left(K^+ K^- + K^- K^+\right) = k(k - 1).$$

To be concrete, for the bilinears in Eq. (7) we identify the vacuum $|0, k\rangle$ as the vacuum Fock state $|0_c\rangle$ of the mode $c$, which fixes $k = 1/4$ since:

$$K_z |0, k\rangle = \frac{1}{2}\left(c^\dagger c + \frac{1}{2}\right) |0_c\rangle = \frac{1}{4} |0_c\rangle . \tag{10}$$

The coherent states in this case are given by displacements of the vacuum Fock state: $|z, 1/4\rangle = \mathcal{D}(z) |0_c\rangle$. (Note that we obtain a second set of SU(1, 1) coherent states by choosing $|0, k\rangle = |1_c\rangle$ which gives $k = 3/4$. One can show that this second set of coherent states is orthogonal to the set generated from $|0_c\rangle$.)

Each SU(1, 1) coherent state is parameterized by a single complex number $z$ with $|z| < 1$, meaning that the coherent states are in one-to-one correspondence with the points of the unit disk as illustrated in Fig. 1.

The SU(1, 1) coherent states are an overcomplete basis for the Hilbert space spanned by the vectors $|n, k\rangle = (K^+)^n |0, k\rangle$. In particular, they are not orthogonal:

$$\langle z, k|z', k\rangle = \frac{(1-|z|^2)^k(1-|z'|^2)^k}{(1-z^*z')^{2k}}. \tag{11}$$

As advertised earlier, the primary advantage of using the coherent states $|z, k\rangle$ is that they transform simply under Hamiltonians composed of SU(1, 1) generators. Specifically, any Hamiltonian of the form (8) will simply transform each coherent state $|z, k\rangle$ into another coherent state $|z', k\rangle$, modulo an unimportant overall phase factor. To see this, consider the dynamics of any state $|\psi(t)\rangle$ under the action of (8). We may write $|\psi(t)\rangle = U(t)|\psi(0)\rangle$ where $U(t)$ is a time-dependent operator that generates the time-evolution of $|\psi(t)\rangle$ and that obeys the Schrödinger equation:

$$\frac{d}{dt}U(t) = -iHU(t)$$

If we parameterize $U(t)$ as:

$$\begin{aligned} U(t) &= e^{z(t)K^+} e^{\ln(1-|z(t)|^2)K_z} e^{-z^*(t)K^-} e^{ig(t)K_z} \\ &= \mathcal{D}(z(t))\ e^{ig(t)K_z} \end{aligned} \tag{12}$$

then one can show by differentiating the exponentiated terms in $U(t)$ that the Schrödinger equation implies the following equations of motion for the coordinates $z(t), g(t)$:

$$\dot{z} = -2i\omega z - i\Omega^* z^2 - i\Omega \tag{13a}$$

$$\dot{g} = -2\omega - 2\mathrm{Re}(\Omega z^*) \tag{13b}$$

Therefore, for an initial state $|\psi(0)\rangle = |0, k\rangle$, the time-evolved state is simply the SU(1, 1) coherent state:

$$|\psi(t)\rangle = e^{ig(t)k}|z(t), k\rangle$$

where $z(t), g(t)$ are solutions to the equations of motion (13). Here we clearly see the benefit of using SU(1, 1) coherent states: the dynamics of the squeezing Hamiltonian (8) is described by a completely classical trajectory, whose equations of motion are given by (13).

More generally, if the initial state $|\psi(0)\rangle = |z_0, k\rangle$ is any SU(1, 1) coherent state, then one can show using standard disentangling theorems that:[17,19]

$$\begin{aligned} |\psi(t)\rangle &= U(t)|z_0, k\rangle \\ &= \mathcal{D}(z(t))\ e^{ig(t)K_z}\ \mathcal{D}(z_0)|0, k\rangle \\ &= e^{if(t)k}\mathcal{D}(z'(t))|0, k\rangle \end{aligned}$$

where $f(t), z'(t)$ are functions of $z(t), z_0$, and $g(t)$ (see Appendix A). We therefore conclude that $|\psi(t)\rangle$ is a coherent state whenever $|\psi(0)\rangle$ is a coherent state and that the dynamics under the Hamiltonian (8) is governed by the completely classical equations of motion (13).

### 3.2 Applications to Spin-Nematic Squeezing

With the SU(1, 1) coherent states at our disposal, we are now in a position to discuss the squeezing dynamics of (8) from a particularly intuitive standpoint. The key connection between the SU(1, 1) coherent states and squeezing is that the displacement operator $\mathcal{D}(z)$ used to generate the coherent states is identical to the single-mode squeezing operator $\mathcal{S}(\alpha)$ commonly found in the quantum optics literature.[13] Specifically, given the bilinears in Eq. (7), one can show using disentangling theorems that:[17,19]

$$\begin{aligned} \mathcal{D}(z) &= e^{zK^+} e^{\ln(1-|z|^2)K_z} e^{-z^*K^-} \\ &= e^{\alpha K^+ - \alpha^* K^-} \\ &= e^{\alpha c^\dagger c^\dagger/2 - \alpha^* cc/2} = \mathcal{S}(-\alpha) \end{aligned} \tag{14}$$

where $\alpha = \tau e^{i\phi}$ and $z = \tanh(\tau)\, e^{i\phi}$. The squeezing operator $\mathcal{S}(\alpha)$ redistributes quantum noise in the two-dimensional phase space spanned by the operators $c, c^\dagger$ as shown in Fig. 3. Introducing canonical coordinates

$$X = (c + c^\dagger)/\sqrt{2} \tag{15a}$$

$$P = (c - c^\dagger)/\sqrt{2}i \tag{15b}$$

for this phase space, and assuming $\alpha \in \mathbb{R}$, the squeezing operator $\mathcal{S}(\alpha)$ reduces noise in the $X$-quadrature by a factor $e^{-\alpha}$ and increases noise in the $P$-quadrature by a factor $e^{\alpha}$. More generally, for complex $\alpha$, the phase of $\alpha$ rotates the orthogonal axes along which quantum noise is squeezed and anti-squeezed.

The utility of the identification (14) is that it provides a direct connection between the coordinate $z$ on the unit disk and the squeezing parameter $\alpha$. From the magnitude of $z$ we can immediately read off the amount of squeezing: in particular, the quantum noise in the squeezed quadrature will be reduced by a factor

$$\xi = e^{-|\alpha|} = \sqrt{(1 - |z|)/(1 + |z|)}. \tag{16}$$

So coordinates $z$ near the edge of the unit disk correspond to highly squeezed states while coordinates close to the center are only mildly squeezed. Furthermore, the phase of $z$ immediately tells us which quadrature is squeezed and which is anti-squeezed. The upshot of all of this is that we can solve for the squeezing dynamics simply by solving the classical equations of motion (13), plotting the resulting classical trajectory for $z(t)$ on the unit disk, and then immediately calculating the amount of squeezing achieved as a function of time using Eq. (16).

To illustrate this explicitly, we solve the classical equations of motion (13) analytically and discuss the resulting squeezing dynamics. The equation of motion for $z(t)$ is a nonlinear Ricatti-type equation, which may be transformed to a second-order differential equation via the substitution:

$$z(t) = -i\frac{dx/dt}{\Omega^* x(t)}$$

which gives:

$$\ddot{x} + 2i\omega\, \dot{x} - |\Omega|^2 x = 0$$

Substituting $x(t) = \psi(t)e^{-i\omega t}$, we obtain

$$\ddot{\psi} + (\omega^2 - |\Omega|^2)\psi = 0$$

whose solutions are $\psi(t) = \sum_\pm \psi_0^\pm e^{\pm\lambda t}$, where $\lambda = \sqrt{|\Omega|^2 - \omega^2}$. Choosing our initial conditions $\psi_0^\pm$ such that $z(0) = 0$, we find a closed-form solution for $z(t)$:

$$z(t) = -i\Omega^3/|\Omega|^2 \, \frac{\sinh \lambda t}{\lambda \cosh \lambda t + i\omega \sinh \lambda t} \tag{17}$$

which depends only on the parameters $\Omega, \omega$ in the Hamiltonian (8). For $\omega < |\Omega|$ we find rapid growth of $z(t)$ toward the boundary of the disk, while for $\omega > |\Omega|$ we find oscillatory behavior where the coordinate $z(t)$ forms closed orbits in the unit disk (see Fig. 2).

While we have focused exclusively on the dynamics generated by the Hamiltonian $H_c$ in the $c, c^\dagger$ phase space, the full Hamiltonian $H = H_c + H_d$ simultaneously generates the same squeezing behavior in the $d, d^\dagger$ phase space as well. Because both terms terms $H_c, H_d$ are governed by the same parameters $\omega, \Omega$, the classical trajectory (17) suffices to describe the dynamics of the entire system.

It is clear from the preceding discussion that the Hamiltonian $H = H_c + H_d$ generates squeezing in the $c, c^\dagger$ and $d, d^\dagger$ subspaces, but in what sense is this equivalent to 'spin-nematic' squeezing observed in spinor BECs? Spin-mixing dynamics are often discussed in the literature in terms of the quadrupole or 'nematic' tensor:[1,4]

$$Q_{ab} = S_a S_b + S_b S_a - (4/3)\delta_{ab} \tag{18}$$

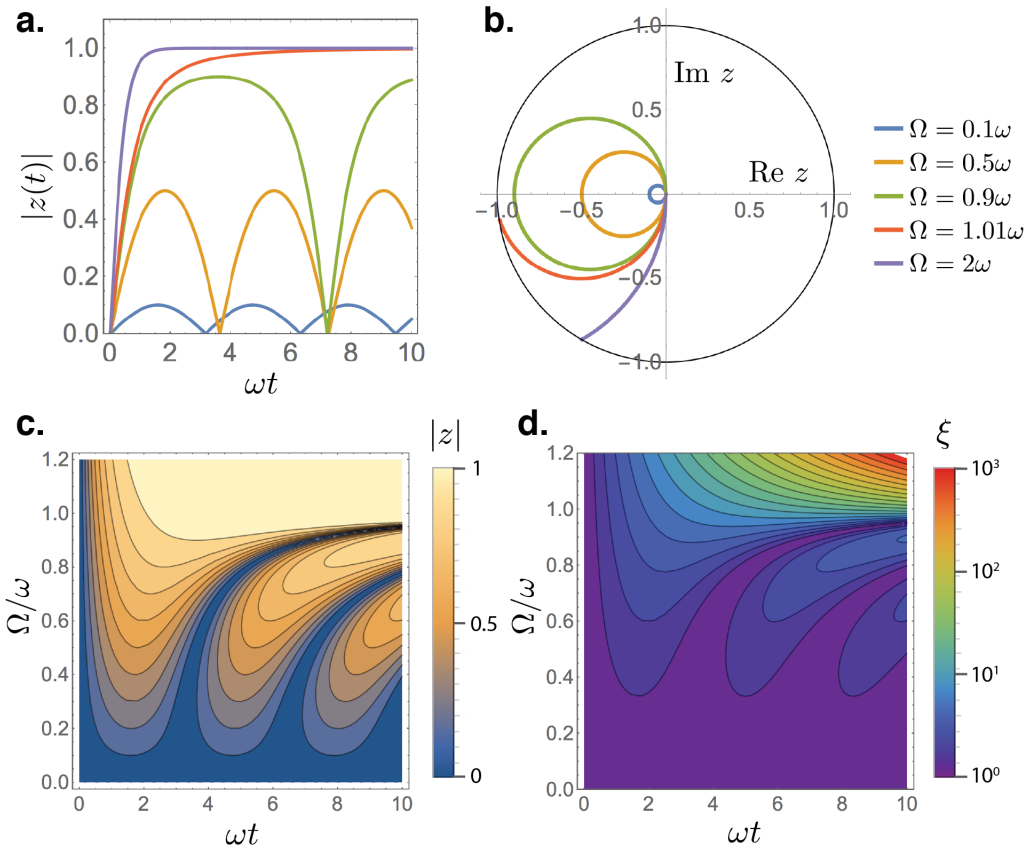


Figure 2. Classical dynamics generated by SU(1, 1) Hamiltonians. (a,b) Starting from the initial state $|0, k\rangle$, one observes either oscillatory (blue, yellow, green) or exponential (red, purple) behavior as a function of the ratio $|\Omega|/\omega$. In (b) we depict the classical trajectories in a parametric plot. All trajectories begin at $z = 0$ and propagate clockwise; oscillatory trajectories return to $z = 0$ while exponential trajectories end on the boundary. (c,d) Motion in the unit disk is equivalent to squeezing in the $c, c^\dagger$ phase space. The radial coordinate $|z|$ (c) gives a direct measure of the amount of squeezing achieved as measured by the squeezing parameter $\xi = \left[\min_\theta 2\left\langle (X\cos\theta + P\sin\theta)^2\right\rangle\right]^{-1/2}$ (d).

where $a, b = \{x, y, z\}$, $S_a$ are components of the total spin vector, and $\delta_{ab}$ is the Kronecker-delta tensor. The nematic tensor is necessary because our system consists of spin-1 objects: while the components of the total spin vector $S_a$ are sufficient to completely describe the state of a spin-1/2 object, for spin-1 objects we must also specify higher moments such as $S_xS_y$, $S_y^2$, etc. The nematic tensor (18) provides a compact way to specify these spin moments. In this language, Hamiltonians of the form (3) generate a redistribution of quantum noise in the subspaces $\mathcal{C} = \{S_x, Q_{yz}, Q_{zz} - Q_{yy}\}$ and $\mathcal{D} = \{S_y, Q_{xz}, Q_{zz} - Q_{xx}\}$,[4,12] hence the name 'spin-nematic' squeezing.

It turns out that the pair of subspaces $\mathcal{C}, \mathcal{D}$ precisely maps onto the pair of subspaces spanned by the operators $c, c^\dagger$ and $d, d^\dagger$ that we have been discussing. To see this, we write the spin and nematic tensor operators in terms of the modes $a_\pm, a_0$, for example:

$$Q_{yz} = \frac{i}{\sqrt{2}}\left(a_+ + a_-\right)a_0^\dagger + \text{h.c.} = ic\,\zeta^* - ic^\dagger\zeta = |\zeta|\,P$$

where in the last step we have assumed $\zeta \in \mathbb{R}$ and substituted the canonical coordinates $X, P$ defined in Eq. (15). (More generally the canonical coordinates $X, P$ will be rotated by the phase of $\zeta$.) Similarly, for $S_x$ and

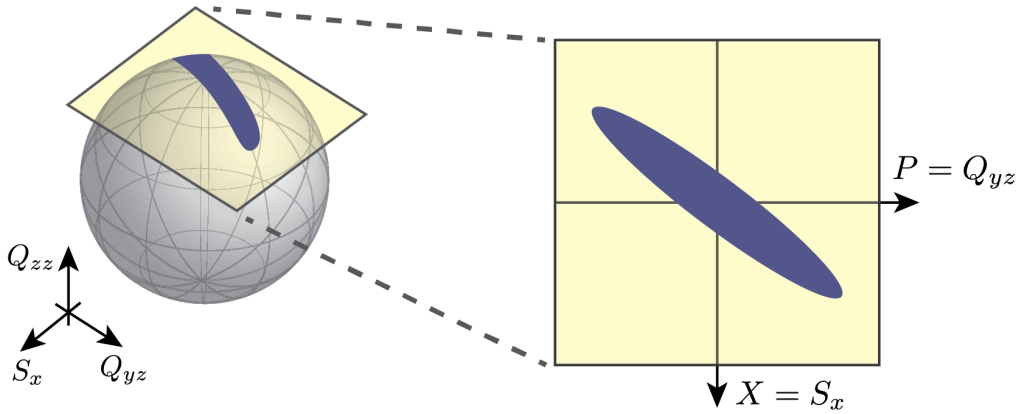


Figure 3. At short times, spin-nematic squeezing dynamics in the subspace $\mathcal{C} = \{S_x, Q_{yz}, Q_{zz} - Q_{yy}\}$ is equivalent to squeezing dynamics in the phase space spanned by $X, P$. This mapping breaks down once the quantum state expands to a significant fraction of the Bloch sphere radius, in which case the curvature of the Bloch sphere becomes important. (Bloch sphere illustration inspired by Hamley, *et al.*[4])

$Q_{zz}$, we find:

$$S_x = |\zeta|\, X$$
$$Q_{zz} - Q_{yy} = c^\dagger c - |\zeta|^2 = \frac{1}{2}\left(X^2 + P^2\right) - |\zeta|^2$$

Therefore, the redistribution of quantum noise in the $X, P$ plane discussed above is equivalent to a redistribution of noise between $S_x$ and $Q_{yz}$ as discussed, for example, by Hamley, *et al.*[4] (see Fig. 3). Similarly, the squeezing occurring in the $d, d^\dagger$ phase space is equivalent to redistribution of noise between $S_y$ and $Q_{xz}$.

The identification of squeezing in the $X, P$ plane with spin-nematic squeezing in the $\{S_x, Q_{yz}, Q_{zz} - Q_{yy}\}$ subspace underscores the limits of the 'classical pump mode' approximation $a_0^\dagger a_0 \approx |\zeta|^2$ we made at the very beginning of this section. As mentioned earlier, this approximation is only valid for short times, when the populations in $a_\pm$ are small compared to $|\zeta|^2$. In taking $|\zeta|^2$ to be large and classical, we are essentially taking the Bloch sphere formed by the SU(2) subgroup $\{S_x, Q_{yz}, Q_{zz} - Q_{yy}\}$ to have a very large radius, and we are only considering the dynamics at the very top of the sphere where the local phase space is approximately flat (see Fig. 3). From this point of view the classical pump mode approximation breaks down precisely when the quantum state has spread out so far that the curvature of the Bloch sphere becomes important. Conversely, the classical pump mode approximation is valid when the quantum state occupies only a small region on the top of the sphere such that it can be reasonably approximated as a flat two-dimensional phase space with canonical coordinates $X = S_x, P = Q_{yz}$.

## 4. EFFECTS OF DISSIPATION

We expect the relaxation operators (6) to spoil the ideal spin-nematic squeezing we have discussed so far. Since dissipation is unavoidable in practice, it will be useful to estimate the maximum amount of squeezing achievable with realistic experimental parameters. Here we find an exact solution for the squeezing dynamics in the presence of dissipation and use it to assess optimal experimental parameters for maximal spin-nematic squeezing.

The dissipative dynamics of the system in the Schrödinger picture are governed by the Lindblad master equation, which takes the form:

$$\dot{\rho} = -i[H, \rho] + \sum_{\pm} L_\pm \rho L_\pm^\dagger - \frac{1}{2} L_\pm^\dagger L_\pm \rho - \frac{1}{2} \rho L_\pm^\dagger L_\pm$$

By multiplying the master equation by an arbitrary operator $\mathcal{O}$ and taking the trace, we immediately obtain an equation of motion for the expectation value of $\mathcal{O}$:

$$\frac{d}{dt}\langle\mathcal{O}\rangle = i\langle[H,\mathcal{O}]\rangle + \sum_{\pm}\left\langle L_{\pm}^{\dagger}\mathcal{O}L_{\pm}\right\rangle - \frac{1}{2}\left\langle L_{\pm}^{\dagger}L_{\pm}\mathcal{O}\right\rangle - \frac{1}{2}\left\langle \mathcal{O}L_{\pm}^{\dagger}L_{\pm}\right\rangle. \tag{19}$$

We may use Eq. (19) to solve for the time-dependence of the variance $(\Delta X')^2$ in the squeezed quadrature $X'$. In general, the squeezed and anti-squeezed quadratures $X', P'$ will be rotated from the axes $X, P$ by an angle $\theta$, which for the moment we leave as a tunable parameter. In terms of the mode operators $c, c^{\dagger}$, we have:

$$\begin{aligned}(\Delta X')^2 &= \left\langle X'^2\right\rangle - \langle X'\rangle^2 \\ &= \left\langle c^{\dagger}c\right\rangle + \frac{1}{2} + \frac{1}{2}\langle cc\rangle e^{-i2\theta} + \frac{1}{2}\left\langle c^{\dagger}c^{\dagger}\right\rangle e^{i2\theta} \\ &\quad - \frac{1}{2}\langle c\rangle^2 e^{-i2\theta} - \frac{1}{2}\left\langle c^{\dagger}\right\rangle^2 e^{i2\theta} - \langle c\rangle\left\langle c^{\dagger}\right\rangle.\end{aligned}$$

Using the equations of motion (19), one can show that for balanced relaxation rates $\gamma_+ \approx \gamma_-$, one obtains a closed set of equations for the expectation values $\left\langle c^{\dagger}c\right\rangle, \langle cc\rangle, \langle c\rangle$ that may be solved exactly. For example, when $\omega = 0$ one finds an explicit expression for the squeezed quadrature at an angle $\theta = \pi/4$:

$$(\Delta X')^2\big|_{\theta=\pi/4} = \frac{1}{2} + \left(\frac{\Gamma}{2|\Omega|} - \frac{1}{2}\right)\left(1 - e^{-2|\Omega|t}\right) \tag{20}$$

where we have introduced $\Gamma = |\zeta|^2(\gamma_+ + \gamma_-)$. At long times, this expression saturates to a minimum variance $(\Delta X')^2 = \Gamma/2|\Omega|$, indicating that the amount of achievable squeezing is ultimately limited by the dissipation rates $\gamma_{\pm}$ as expected.

To minimize these dissipative effects, one can increase the detuning of the drive light from cavity resonance in order to decrease the spin relaxation rates $\gamma_{\pm}$. In the limit of large drive detuning, however, the interaction rate $\Omega$ also slows down and one must ultimately contend with atomic scattering into free space at a rate proportional to the atomic linewidth. As a result, one must choose an intermediate drive detuning that strikes a compromise between the two competing forms of dissipation arising from cavity decay and atomic free-space scattering. One can show that the optimal drive detuning gives an interaction-to-decay ratio that scales as:[20]

$$\frac{|\Omega|}{\Gamma} \sim \sqrt{N\eta} \tag{21}$$

where $N$ is the total atom number and $\eta$ is the single-atom cooperativity. Combining this result with Eq. (20) we conclude that a cavity QED system, including dissipation, is capable of reducing quantum noise in the spin-nematic squeezed quadrature by up to a factor $(\Delta X')^2 \sim 1/\sqrt{N\eta}$.

## 5. EFFECTS OF NON-UNIFORM CAVITY COUPLING

Thus far, we have assumed that all atoms are coupled uniformly to the cavity mode (i.e. $\xi_i = 1$ for all $i$). Realistically, however, the couplings $\xi_i$ can vary over the length of the atomic ensemble by as much as a factor of 2, which in principle can have a substantial impact on the resulting dynamics. To understand the effect of this non-uniformity, we map the Hamiltonian (1) onto a hard-core boson model that retains the non-uniform coupling and allows us to analyze the resulting dynamics.

For each atom $i$, we introduce two bosonic modes $a_i, b_i$ and associate each of the spin-1 atomic states with a Fock state of these modes as follows:

$$|0_a, 0_b\rangle = |m_F = 0\rangle \tag{22a}$$
$$|1_a, 0_b\rangle = |m_F = +1\rangle \tag{22b}$$
$$|0_a, 1_b\rangle = |m_F = -1\rangle \tag{22c}$$

We then impose hard-core constraints on the bosons such that the energy penalty $U$ for placing two bosons in a single mode (e.g. $|2_a, 0_b\rangle$) is prohibitively high. This restricts the low-energy subspace to the three $m_F$ levels in (22), plus a fourth state $|X\rangle = |1_a, 1_b\rangle$, which decouples from the dynamics.

Using these bosonic operators, the spin-spin Hamiltonian (1) therefore maps exactly to the boson model:

$$H = 2\chi \sum_{ij} \xi_i \xi_j \left(a_i^\dagger + b_i\right)\left(a_j + b_j^\dagger\right) + q\sum_i \left(a_i^\dagger a_i + b_i^\dagger b_i\right) + U\sum_i a_i^\dagger a_i^\dagger a_i a_i + U\sum_i b_i^\dagger b_i^\dagger b_i b_i \tag{23}$$

in the limit $U \to \infty$. The utility of this mapping is that the system at early times contains very few bosons, so the hardcore constraints may be ignored. This is essentially a dilute gas approximation at lowest order, and in principle we could do a controlled approximation in powers of the boson density to compute corrections to this approximation.

In the absence of the hardcore constraints, we can explicitly diagonalize the Hamiltonian (23) by transforming to a new set of modes

$$\mathcal{A} = \frac{1}{\sqrt{\Phi}}\sum_i \xi_i a_i$$
$$\mathcal{B} = \frac{1}{\sqrt{\Phi}}\sum_i \xi_i b_i$$

where $\Phi = \sum_i \xi_i^2$. In terms of these non-uniform bosonic modes, the Hamiltonian takes the form:

$$H = 2\chi\Phi\left(\mathcal{A}^\dagger + \mathcal{B}\right)\left(\mathcal{A} + \mathcal{B}^\dagger\right) + q\mathcal{Q} \tag{24}$$

where $\mathcal{Q} = \sum_i a_i^\dagger a_i + b_i^\dagger b_i$ is the total number of excitations in the side modes. The mode operators $\mathcal{A}, \mathcal{B}$ obey the usual commutation relations:

$$\left[\mathcal{A}, \mathcal{A}^\dagger\right] = 1$$
$$\left[\mathcal{B}, \mathcal{B}^\dagger\right] = 1$$

while $\mathcal{Q}$ behaves like a number operator:

$$[\mathcal{Q}, \mathcal{A}] = -\mathcal{A}$$
$$[\mathcal{Q}, \mathcal{B}] = -\mathcal{B}.$$

Furthermore, one can show that

$$\mathcal{N} = \mathcal{A}^\dagger\mathcal{A} + \mathcal{B}^\dagger\mathcal{B} + 1 - \mathcal{Q} \tag{25}$$

is a constant of motion.

Using these commutation relations, one can explicitly solve for the dynamics of the side mode population $\mathcal{Q}$:

$$\frac{d}{dt}\mathcal{Q} = 4i\chi\Phi\left(\mathcal{A}\mathcal{B} - \mathcal{A}^\dagger\mathcal{B}^\dagger\right)$$
$$\frac{d}{dt}\left(\mathcal{A}\mathcal{B} - \mathcal{A}^\dagger\mathcal{B}^\dagger\right) = -4i\chi\Phi\left(\mathcal{A}^\dagger\mathcal{A} + \mathcal{B}^\dagger\mathcal{B} + 1\right) - 2i\left(q + 2\chi\Phi\right)\left(\mathcal{A}\mathcal{B} + \mathcal{A}^\dagger\mathcal{B}^\dagger\right)$$

We can combine these two equations and write them in terms of the constants of motion $\mathcal{N}, H$ to obtain:

$$\frac{d^2}{dt^2}\mathcal{Q} = -8\chi\Phi\left(q\mathcal{N} - \frac{q + 2\chi\Phi}{2\chi\Phi}H\right) - 4\left(q + 4\chi\Phi\right)q\mathcal{Q} \tag{26}$$

whose solutions are linear combinations of $\cosh\lambda t, \sinh\lambda t$, where

$$\lambda = 2\sqrt{-q(q + 4\chi\Phi)} \tag{27}$$

For equal couplings $\xi_i = 1$, this is exactly the same exponential growth rate we obtain from a mean-field treatment with a classical pump. In this case the sum over weights $\Phi = \sum_i \xi_i^2$ is just equal to the total atom number and plays the role of the initial pump population $|\zeta|^2$. For non-uniform couplings, the factor $\Phi$ decreases in a way that depends both on the average coupling and the variance in the couplings.

Despite decreasing the exponential growth rate $\lambda$, we speculate that the presence of non-uniform couplings $\xi_i$ may present opportunities for quantum-enhanced metrology. While spin-nematic squeezed states produced by uniformly-coupled atomic ensembles are most sensitive to global rotations and displacements in phase space, we expect that the sensitivity of the modes $\mathcal{A}, \mathcal{B}$ will be modulated by the coupling coefficients $\xi_i$, which may be controlled by driving the cavity from the side with non-uniform drive light. This inhomogeneity in sensitivity could be leveraged, for instance, to perform quantum-enhanced measurements of inhomogeneous magnetic fields with a tunable spatial dependence governed by the couplings $\xi_i$. We leave a detailed investigation of this possibility to future work.

## 6. CONCLUSION

In this paper we studied the spin-mixing dynamics generated in a driven cavity QED setup from several perspectives. In the absence of dissipation we showed that the dynamics can be understood in terms of the generators of the Lie group SU(1, 1). We introduced a set of SU(1, 1) coherent states that transform the dynamics into a completely classical problem, with equations of motion given by Eq. (13). We also showed how these coherent states relate to discussions of spin-nematic squeezing often found in the literature. In addition, we found analytic expressions for the squeezing dynamics in the presence of dissipation and estimated the maximal squeezing achievable in realistic cavity systems. Finally, we discussed modifications to the dynamics generated by non-uniform coupling to the cavity mode.

Due to its versatility and tunability, we anticipate that cavity QED platforms will allow both corroboration of and extensions to the rich set of spin-mixing phenomena observed in spinor BECs. One new possibility is to tune the system across the ferro-/antiferro-magnetic phase transition, which is inherently inaccessible in spinor Bose gases. In addition, using tools such as non-uniform atom-cavity coupling and non-uniform drive fields, we expect to access many-body dynamics beyond the mean-field approximation. Moreover, breaking the all-to-all uniformity may also allow for the preparation of metrological states that could be used for quantum-enhanced imaging.

## APPENDIX A. COMPOSITION OF SU(1, 1) DISPLACEMENTS

Here we show that SU(1, 1) Hamiltonians transform SU(1, 1) coherent states into coherent states. First, we show that the composition of two SU(1, 1) displacements is equivalent to a rotation followed by an SU(1, 1) displacement:

$$\mathcal{D}(x)\mathcal{D}(y) = \mathcal{D}(z)\exp\left[ihK_z\right] \tag{28}$$

where

$$\mathcal{D}(z) = e^{zK^+}e^{\ln(1-|z|^2)K_z}e^{-z^*K^-}.$$

The simplest way to show this equivalence is to represent the SU(1, 1) generators using a (non-unitary) $2 \times 2$ matrix representation:[17]

$$K_x = \frac{i}{2}\sigma_y$$
$$K_y = -\frac{i}{2}\sigma_x$$
$$K_z = \frac{1}{2}\sigma_z$$

where $\vec{\sigma}$ are the Pauli matrices. In this representation,

$$\mathcal{D}(z) = \frac{1}{\sqrt{1-|z|^2}}\begin{bmatrix} 1 & z^* \\ -z & 1 \end{bmatrix} \tag{29}$$

and

$$\exp\left[ihK_z\right] = \begin{bmatrix} e^{ih/2} & 0 \\ 0 & e^{-ih/2} \end{bmatrix}. \tag{30}$$

Similarly, Eq. (28) becomes:

$$\frac{1}{\sqrt{1-|x|^2}}\frac{1}{\sqrt{1-|y|^2}}\begin{bmatrix} 1-yx^* & x^*+y^* \\ -x-y & 1-y^*x \end{bmatrix} = \frac{1}{\sqrt{1-|z|^2}}\begin{bmatrix} e^{ih/2} & z^*e^{-ih/2} \\ -ze^{ih/2} & e^{-ih/2} \end{bmatrix}$$

which gives a set of 3 equations for 3 real unknowns that allow us to solve for $z, h$ in terms of $x, y$. Explicitly:

$$|z|^2 = 1 - \frac{(1-|x|^2)(1-|y|^2)}{(1-yx^*)(1-y^*x)} \tag{31a}$$

$$\mathrm{Arg}\left[z\right] + \frac{h}{2} = \mathrm{Arg}\left[x+y\right] \tag{31b}$$

$$h = 2\mathrm{Arg}\left[1-yx^*\right] \tag{31c}$$

Because this $2\times 2$ matrix representation is a faithful representation of $\mathrm{SU}(1,1)$, we conclude that the operator equation (28) must hold for *any* representation, and therefore that it holds as an operator equality.

Having shown (28), we may also conclude that $\mathrm{SU}(1,1)$ Hamiltonians preserve $\mathrm{SU}(1,1)$ coherent states. In the main text, we argued that arbitrary states evolve under any $\mathrm{SU}(1,1)$ Hamiltonian evolve as $|\psi(t)\rangle = U(t)\,|\psi(0)\rangle$ where the evolution operator $U(t)$ takes the form in Eq. (12). Suppose that $|\psi(0)\rangle$ is a $\mathrm{SU}(1,1)$ coherent state:

$$|\psi(0)\rangle = \mathcal{D}(z_0)\,|0,k\rangle\,.$$

The time-evolved state is then:

$$\begin{aligned} |\psi(t)\rangle &= \mathcal{D}(z(t))\exp\left[ig(t)K_z\right]\mathcal{D}(z_0)\,|0,k\rangle \\ &= \mathcal{D}(z(t))\mathcal{D}(z'(t))\exp\left[ig(t)K_z\right]|0,k\rangle \\ &= \mathcal{D}(\overline{z}(t))\exp\left[i(h(t)+g(t))K_z\right]|0,k\rangle \\ &= e^{ik(h(t)+g(t))}\,|\overline{z}(t),k\rangle \end{aligned}$$

where in the second line we have inserted factors of $\exp\left[\pm ig(t)K_z\right]$ on the right such that $z'(t) = z_0 e^{ig(t)}$, and in the third line we have used (28). We therefore conclude that, aside from an unimportant phase factor, coherent states are transformed to coherent states under the action of $\mathrm{SU}(1,1)$ Hamiltonians. If the initial state is $|\psi(0)\rangle = |0,k\rangle$ then the above result is even simpler: we find

$$|\psi(t)\rangle = e^{ikg(t)}\,|z(t),k\rangle\,.$$

So if we solve the classical equations of motion (13), we therefore also solve for the exact quantum dynamics of the system.

## ACKNOWLEDGMENTS

This work was supported by the DOE Office of Science. G.S.B. acknowledges support from the NSF GRFP. E.J.D. acknowledges support from the Hertz Foundation and NSF GRFP. L.H. was supported by the Max Weber Foundation. A.P. and E.C. acknowledge support from the NSF under grant No. PHY-1753021. M.S-S. acknowledges support from the Research Corporation Cottrell Scholar program.

## REFERENCES


[1] Stamper-Kurn, D. M. and Ueda, M., "Spinor bose gases: symmetries, magnetism, and quantum dynamics," *Reviews of Modern Physics* **85**, 1191–1244 (2013).

[2] Leslie, S. R., Guzman, J., Vengalattore, M., Sau, J. D., Cohen, M. L., and Stamper-Kurn, D. M., "Amplification of fluctuations in a spinor Bose-Einstein condensate," *Physical Review A* **79**(4), 043631 (2009).

[3] Klempt, C., Topic, O., Gebreyesus, G., Scherer, M., Henninger, T., Hyllus, P., Ertmer, W., Santos, L., and Arlt, J. J., "Parametric amplification of vacuum fluctuations in a spinor condensate," *Physical Review Letters* **104**(19), 195303 (2010).

[4] Hamley, C. D., Gerving, C. S., Hoang, T. M., Bookjans, E. M., and Chapman, M. S., "Spin-nematic squeezed vacuum in a quantum gas," *Nature Physics* **8**(4), 305–308 (2012).

[5] Linnemann, D., Strobel, H., Muessel, W., Schulz, J., Lewis-Swan, R. J., Kheruntsyan, K. V., and Oberthaler, M. K., "Quantum-enhanced sensing based on time reversal of nonlinear dynamics," *Physical Review Letters* **117**(1), 013001 (2016).

[6] Chang, M.-S., Hamley, C. D., Barrett, M. D., Sauer, J. A., Fortier, K. M., Zhang, W., You, L., and Chapman, M. S., "Observation of spinor dynamics in optically trapped $^{87}$Rb Bose-Einstein condensates," *Physical Review Letters* **92**, 140403 (2004).

[7] Guzman, J., Jo, G.-B., Wenz, A. N., Murch, K. W., Thomas, C. K., and Stamper-Kurn, D. M., "Long-time-scale dynamics of spin textures in a degenerate $F = 1$ $^{87}$Rb spinor Bose gas," *Physical Review A* **84**, 063625 (2011).

[8] Bookjans, E. M., Vinit, A., and Raman, C., "Quantum phase transition in an antiferromagnetic spinor Bose-Einstein condensate," *Physical Review Letters* **107**, 195306 (2011).

[9] Sadler, L. E., Higbie, J. M., Leslie, S. R., Vengalattore, M., and Stamper-Kurn, D. M., "Spontaneous symmetry breaking in a quenched ferromagnetic spinor Bose-Einstein condensate," *Nature* **443**(7109), 312–315 (2006).

[10] Luo, X.-Y., Zou, Y.-Q., Wu, L.-N., Liu, Q., Han, M.-F., Tey, M. K., and You, L., "Deterministic entanglement generation from driving through quantum phase transitions," *Science* **355**(6325), 620–623 (2017).

[11] Davis, E. J., Bentsen, G., Homeier, L., Li, T., and Schleier-Smith, M. H., "Photon-mediated spin-exchange dynamics of spin-1 atoms," *Physical Review Letters* **122**, 010405 (2019).

[12] Masson, S. J., Barrett, M. D., and Parkins, S., "Cavity QED engineering of spin dynamics and squeezing in a spinor gas," *Physical Review Letters* **119**(21), 213601 (2017).

[13] Caves, C. M. and Schumaker, B. L., "New formalism for two-photon quantum optics. I. Quadrature phases and squeezed states," *Physical Review A* **31**, 3068–3092 (1985).

[14] Perelomov, A. M., "Coherent states for arbitrary Lie group," *Communications in Mathematical Physics* **26**(3), 222–236 (1972).

[15] Gerry, C. C., "Dynamics of SU(1,1) coherent states," *Physical Review A* **31**(4), 2721–2723 (1985).

[16] Bechler, A., "Compact and noncompact dynamics of the SU(1, 1) coherent states driven by a coherence preserving Hamiltonian," *Journal of Physics A: Mathematical and General* **34**(39), 8081–8100 (2001).

[17] Arecchi, F. T., Courtens, E., Gilmore, R., and Thomas, H., "Atomic coherent states in quantum optics," *Physical Review A* **6**, 2211–2237 (1972).

[18] Bargmann, V., "Irreducible unitary representations of the Lorentz group," *Annals of Mathematics* **48**(3), 568 (1947).

[19] Ban, M., "Decomposition formulas for su(1, 1) and su(2) Lie algebras and their applications in quantum optics," *Journal of the Optical Society of America B* **10**(8), 1347 (1993).

[20] Davis, E., Bentsen, G., and Schleier-Smith, M., "Approaching the heisenberg limit without single-particle detection," *Phys. Rev. Lett.* **116**, 053601 (2016).

[21] Zhao, L., Tang, T., Chen, Z., and Liu, Y., "Lattice-induced rapid formation of spin singlets in spin-1 spinor condensates," *arXiv preprint* , arXiv:1801.00773 (2018).

[22] Zhang, W., Zhou, D. L., Chang, M.-S., Chapman, M. S., and You, L., "Coherent spin mixing dynamics in a spin-1 atomic condensate," *Physical Review A* **72**(1), 013602 (2005).

[23] Lücke, B., Scherer, M., Kruse, J., Pezzé, L., Deuretzbacher, F., Hyllus, P., Topic, O., Peise, J., Ertmer, W., Arlt, J., Santos, L., Smerzi, A., and Klempt, C., "Twin matter waves for interferometry beyond the classical limit," *Science* **334**(6057), 773–776 (2011).